Biomechanical Impact of Localized Corneal Cross-linking Beyond the Irradiated Treatment Area

Joshua N. Webb, BS; Erin Langille; Farhad Hafezi, MD, PhD; J. Bradley Randleman, MD; Giuliano Scarcelli, PhD

ABSTRACT

PURPOSE: To investigate the stiffening effect of localized corneal cross-linking (L-CXL) within and beyond the irradiated region in three dimensions.

METHODS: Ten porcine eyes were debrided of epithelium and incrementally soaked with 0.1% riboflavin solution. Using a customized, sharp-edged mask, half of the cornea was blocked while the other half was exposed to blue light (447 nm). The three-dimensional biomechanical properties of each cornea were then measured via Brillouin microscopy. An imaging system was used to quantify the optimal transition zone between cross-linked and non-cross-linked sections of the cornea when considering light propagation and scattering.

RESULTS: A broad transition zone of 610 µm in width was observed between the fully cross-linked and non-cross-linked sections, indicating the stiffening response extended beyond the irradiated region. Light propagation and the scattering induced by the riboflavin-soaked cornea accounted for a maximum of 25 and 159 ± 3.2 µm, respectively.

CONCLUSIONS: The stiffening effect of L-CXL extends beyond that of the irradiated area. When considering L-CXL protocols clinically, it will be important to account for increased stiffening in surrounding regions.

[*J Refract Surg*. 2019;35(4):253-260.]

Corneal ectasia, the second leading cause of corneal transplantation worldwide,[1] is characterized by alterations in corneal morphology due to a non-uniform decrease in the stiffness of the cornea.[2-4] The U.S. Food and Drug Administration has recently approved corneal cross-linking (CXL) to halt the ectatic process by stiffening the cornea. The procedure calls for soaking the cornea with a photosensitizer (riboflavin) followed by uniform ultraviolet-A (UV-A) exposure.[5-7] When riboflavin is exposed to UV light in an oxygenated environment, reactive oxygen species are formed.[6] This leads to the creation of additional chemical bonds throughout the corneal tissue collagen, thereby increasing overall corneal strength.[8-10]

Localized CXL (L-CXL) has recently been proposed to address the spatially dependent characteristics of ectasia.[11-13] By limiting the irradiated area, the risk of complication and infection is expected to diminish due to less epithelial removal,[14] potential haze, and stromal damage.[12] Most important, because the stiffen-

From Fischell Department of Bioengineering, University of Maryland, College Park, Maryland (JNW, EL, GS); Laboratory for Ocular Cell Biology, Center for Applied Biotechnology and Molecular Medicine, University of Zurich, Switzerland (FH, JBR); ELZA Institute, Dietikon, Switzerland (FH); Faculty of Medicine, University of Geneva, Geneva, Switzerland (FH); the Department of Ophthalmology, University of Wenzhou, Wenzhou, China (FH); and USC Roski Eye Institute (FH, JBR) and Keck School of Medicine (JBR), University of Southern California, Los Angeles, California.

Submitted: December 23, 2018; Accepted: March 4, 2019

Supported in part by NIH Grant No. R01 EY028666 and an unrestricted departmental grant to the USC Roski Eye Institute from Research to Prevent Blindness, Inc.

Dr. Hafezi is a shareholder/investor for EMAGine AG (Zug, Switzerland), a consultant for GroupAdvance Consulting GmbH (Zug, Switzerland), an exclusive patent owner for PCT patent/application (corneal apparatus used for CXL and chromophore for CXL application), and a recipient of travel funds from Light for Sight Foundation (Zurich, Switzerland), directed research funds from Light for Sight Foundation (Zurich, Switzerland), SCHWIND eye-tech-solutions (Kleinostheim, Germany), VELUX Foundation (Søborg, Denmark), Gelbert Foundation (Geneva, Switzerland), and in-kind financial contribution for research materials from SOOFT Italia (Montegiorgio, Italy). Dr. Scarcelli is a consultant for Intelon Optics. The remaining authors have no financial or proprietary interest in the materials presented herein.

Dr. Randleman did not participate in the editorial review of this manuscript.

Correspondence: Giuliano Scarcelli, PhD, University of Maryland, 4228 A. James Clark Hall, College Park, MD 20742. E-mail: scarc@umd.edu

doi:10.3928/1081597X-20190304-01

TABLE 1
CXL Methods

Parameter	Variable (UV-A Light)	Variable (Blue Light)
Treatment target	Ectasia	Ectasia
Fluence (total) (J/cm^2)	5.4	18
Soak time and interval (minutes)	20 (q3)	20 (q3)
Intensity (mW)	9	15
Treatment time (minutes)	10	20
Epithelium status	Off	Off
Chromophore	Riboflavin	Riboflavin
Chromophore carrier	Dextran	Dextran
Chromophore osmolarity	Iso-osmolar	Iso-osmolar
Chromophore concentration	0.1%	0.1%
Light source	UVA (365nm) UV Curing LED System (Thorlabs, Newton, NJ)	Blue (447nm) Diode Laser (Opto Engine LLC, Salt Lake City, UT)
Irradiation mode (interval)	Continuous	Continuous
Protocol modifications	Blocking mask	Blue laser light, Blocking mask
Protocol abbreviation in manuscript	UV-A L-CXL (Localized)	Blue light L-CXL (Localized)

CXL= corneal cross-linking; UV-A = ultraviolet

ing is concentrated in the mechanically compromised area of the cornea, greater local topographical flattening is expected.[15] However, the biomechanical properties of the cornea after L-CXL procedures have not yet been evaluated due to the lack of characterization methods capable of measuring corneal mechanical properties with three-dimensional resolution.

The purpose of this study was to non-invasively measure and characterize the spatial distribution of the modulus of the cornea following L-CXL using Brillouin microscopy and determine the magnitude and extent of the stiffening effect from CXL beyond the irradiated (UV-A exposed) region of the cornea.

MATERIALS AND METHODS

Freshly enucleated porcine eyes were obtained from a local slaughterhouse. They were kept in ice during the transportation until the start of the experiment. The experiment was completed within 8 hours after the animal was killed. All corneas with intact epithelium were visually inspected to avoid using damaged or unclear tissue prior to any experimentation. L-CXL was performed ex vivo by restricting illumination during CXL to half the porcine cornea using a customized mask. The procedure was performed using a traditional UV protocol and a protocol using blue light.

UV-A L-CXL

To illustrate the issue, we performed the UV-A L-CXL experiment on one porcine eye after epithelial debridement followed by the administration of one drop of 0.1% riboflavin solution every 3 minutes for 20 minutes. Next, a constant UV-A (365-nm) power of 9 mW/cm^2 was applied via a high-power UV Curing LED System (Thorlabs, Newton, NJ) for 10 minutes.[9,16,17] Because the primary purpose of the UV light experiment was to illustrate the spatial variation of the CXL procedure and to minimize any potential variation in tissue hydration, an accelerated protocol was chosen and implemented. Half of the cornea was blocked from UV light using a homemade, sharp-edged mask placed directly above the anterior of the cornea. During UV light exposure, one drop of riboflavin solution was administered to the cornea at 5-minute intervals. The UV L-CXL methods are outlined in **Table 1**. Using Brillouin microscopy, we analyzed the biomechanical properties of the sample in three dimensions and calculated the transition zone.

Blue Light L-CXL

Because the UV-A lamp is an extended source emitting incoherent light, it was reasonable to assume that radiation could not be confined to sharp transitions; thus, we used a blue laser and validated a CXL protocol using blue light.

For the blue light L-CXL experiment, 10 porcine eyes had epithelial debridement followed by the administration of one drop of 0.1% riboflavin solution every 3 minutes for 20 minutes. Similar to previous experiments performing blue light CXL,[18,19] the cornea

was then exposed to 15 mW/cm^2 blue light (447-nm) radiation for 20 minutes via a blue diode laser light source (Opto Engine LLC, Salt Lake City, UT). During blue light exposure, one drop of riboflavin solution was applied at 5-minute intervals. In a manner similar to UV-A L-CXL, the blue light procedure was localized using the blocking mask. The blue light L-CXL methods are outlined in **Table 1**.

Using Brillouin microscopy, we analyzed the biomechanical properties of each sample and calculated each transition zone. We aligned the transition zones of the corneas at 50% respective normalized stiffness and averaged across the depth axis.

Brillouin Microscopy

A confocal Brillouin microscope was used with a configuration similar to previous studies[9,20-23] but at a different incident wavelength. Briefly, a 660-nm laser with an optical power of 15 mW was focused into the sample by a 40× objective lens with a numerical aperture of 0.6 (Olympus), a transverse resolution of approximately 1 µm, and a depth resolution of approximately 2 µm. The scattered light, collected through the same objective, was coupled into a single mode fiber and delivered to a two-stage virtually imaged-phase-array (VIPA) spectrometer featuring an electron multiplying charge coupled device (EMCCD) camera (Andor, IXon Du-897; Belfast, United Kingdom). Each Brillouin spectrum was acquired in 0.15 second. To quantify the Brillouin shift at each sample location, raw spectra from the camera were fitted using a Lorentzian function and calibrated using the known frequency shifts of water and glass.

From the Brillouin frequency shift, the local mechanical properties of the cornea can be estimated using the following formula:

$$M' = \frac{\rho {\nu_B}^2 {\lambda_i}^2}{4n^2}$$

where M' is the Brillouin-derived longitudinal modulus, υ_B is the measured Brillouin frequency shift, n is the refractive index of the material, λ_i is the wavelength of the incident photons, and ρ is the density of the material. The spatially varying ratio of ρ/n^2 was approximated to the constant value of 0.57 g/cm^3 based on values in the literature[18,24]; we estimate this to introduce a 0.3% uncertainty throughout the cornea.[25,26] Previously, we have validated the strong relationship ($R > 0.9$) between the Brillouin-derived modulus and the Young's modulus found via gold-standard stress-strain compression tests on porcine corneas.[9]

Calculation of Transition Zones

The primary metric quantified in this study was the transition zone between the fully irradiated and non-irradiated corneal areas. A sharp-edged mask was used throughout the protocols to define the two sections. Although several different parameters were evaluated, including light intensity and Brillouin modulus, a common computation of the transition zone was conducted on each respective image.

To calculate the transition zone, the light intensity was averaged along the perpendicular axis normal to the transition edge and normalized using the equation:

$$[I_n] = \frac{([I] - [I_{min}])}{([I_{max}] - [I_{min}])}$$

where I_n is the normalized intensity, I is the average measured intensity, and I_{min} and I_{max} are the intensities at the lowest and greatest plateau, respectively. We calculated the transition zone as the distance between 10% and 90% of the maximum value. Only the anterior one-third of the cornea was used for analysis of the transition zone of CXL procedures because that was the region primarily affected by L-CXL.[9,27] For Brillouin maps, the Brillouin modulus was used in place of light intensity throughout the calculation of the transition zone.

Biomechanical Testing

To validate the blue light protocol, we compared the Young's modulus of control and blue light CXL buttons punched from the same respective cornea. Eight porcine corneas were dissected. Two 5-mm central corneal disc samples were created (Disposable Biopsy Punch; Integra Miltex, Plainsboro, NJ) from each cornea. Both disc samples were treated; with one drop of 0.1% riboflavin solution every 3 minutes for 20 minutes. One of the two samples was set aside as the control and the other sample was fully exposed to 15 mW/cm^2 blue light radiation for 20 minutes. During the irradiation process, hydration of both the control and exposed discs was maintained via the application of one drop of riboflavin solution at 5-minute intervals.

Next, mechanical properties of each sample were tested using a Microsquisher compressive stress-strain instrument (model: MT G2) and the associated Squisherjoy software (Cellscale, Waterloo, Ontario, Canada). The instrument directly compressed the corneal samples using a 6 × 6 mm plate attached to a 0.5588-mm diameter microbeam. To obtain the Young's modulus of a sample, the Stress (Force/Area) vs Strain (Displacement/Thickness) curve was obtained and the slope of the linear segment of the curve

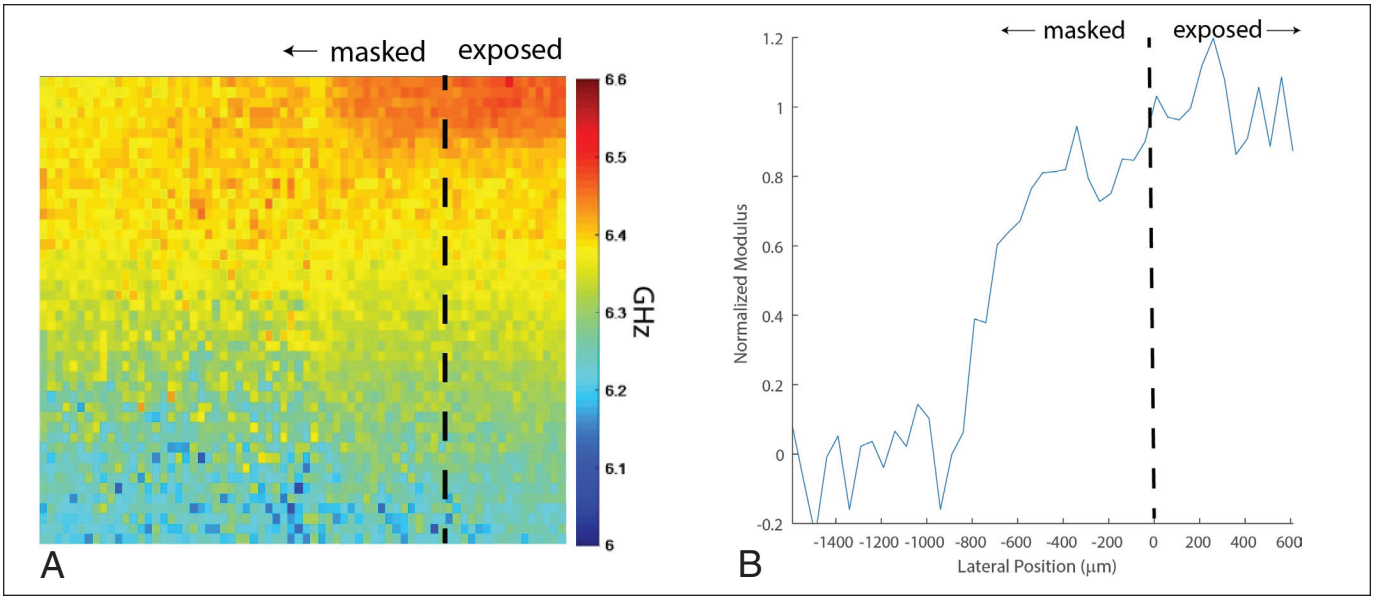

Figure 1. (A) Representative Brillouin map (4,000 × 700 μm) produced with MATLAB software (Mathworks, Natick, MA) (color map: jet) depicting the Brillouin shifts of an ultraviolet (UV)-induced, locally cross-linked porcine cornea positioned anterior up. The dotted line illustrates the edge of the UV blocking mask, differentiating the blocked and exposed sections of the cornea. A higher Brillouin shift correlates to a higher Brillouin modulus. (B) The normalized Brillouin modulus versus lateral position. Similar to 1A, the dotted line illustrates the edge of the UV blocking mask. The transition zone was taken as 10% to 90% normalized modulus.

following the sleek strain was quantified. For each sample, we reported the modulus at 1.5% to 4.5% strain.

Measurement of Light Propagation From Blue Light L-CXL Set-up

To isolate the transition zone generated by the blue light source alone, using the blue light L-CXL set-up, we replaced the corneal sample with a complementary metal–oxide–semiconductor (CMOS) camera (Mightex Systems, Toronto, Ontario, Canada). The camera has a 1,280 × 1,024 monochrome resolution with 5.2 μm per pixel and 50 ms exposure time. To quantify the light exposure at the varying depths of the cornea, we placed the camera at a distance 0, 500, and 1,000 μm from the mask; 0 μm to represent the anterior surface and 1,000 μm to represent the posterior edge at the estimated maximum porcine corneal thickness. At the three distances, respective images were captured and the light transition zone was calculated.

Measurement of Light Scattering Within the Cornea

Light scattering within the cornea could result in riboflavin outside of the directly irradiated area becoming excited, and therefore CXL surrounding cornea that is otherwise covered by the mask. To measure light scattering throughout the L-CXL procedure, we mimicked the blue light L-CXL set-up at three conditions. First, we replaced the cornea with a CMOS camera at a distance 3 mm from the mask. Respective images (n = 7) were taken and transition zones calculated based on measured light intensity. Following each image capture, we placed a 5-mm punched porcine corneal disc on top of the CMOS camera. Under the same conditions, images were captured and analyzed. Finally, we subjected punched discs (n = 4) to one drop of 0.1% riboflavin solution every 3 minutes for 20 minutes. We then placed the cornea on the camera, captured respective images, and similarly analyzed the riboflavin/cornea transition zone.

Statistical Analysis

For gold standard biomechanical analysis, the Young's modulus of samples extracted from the same cornea were calculated as previously indicated and compared using a Wilcoxon signed-rank test. To compare the corneal scattering–induced transition zones to their respective controls, we performed a Wilcoxon signed-rank test. To compare the scattering-induced transition zones of riboflavin-soaked corneas to virgin corneas and cornea-omitted controls, a Mann–Whitney *U* test was performed.

RESULTS

Figure 1A shows the Brillouin map of a UV-induced, locally cross-linked cornea. Brillouin microscopy revealed two distinct lateral regions within the cornea that extend the entire depth: a fully cross-linked section and a non-cross-linked section. The two regions primarily varied in anterior stiffness. Importantly, these sections

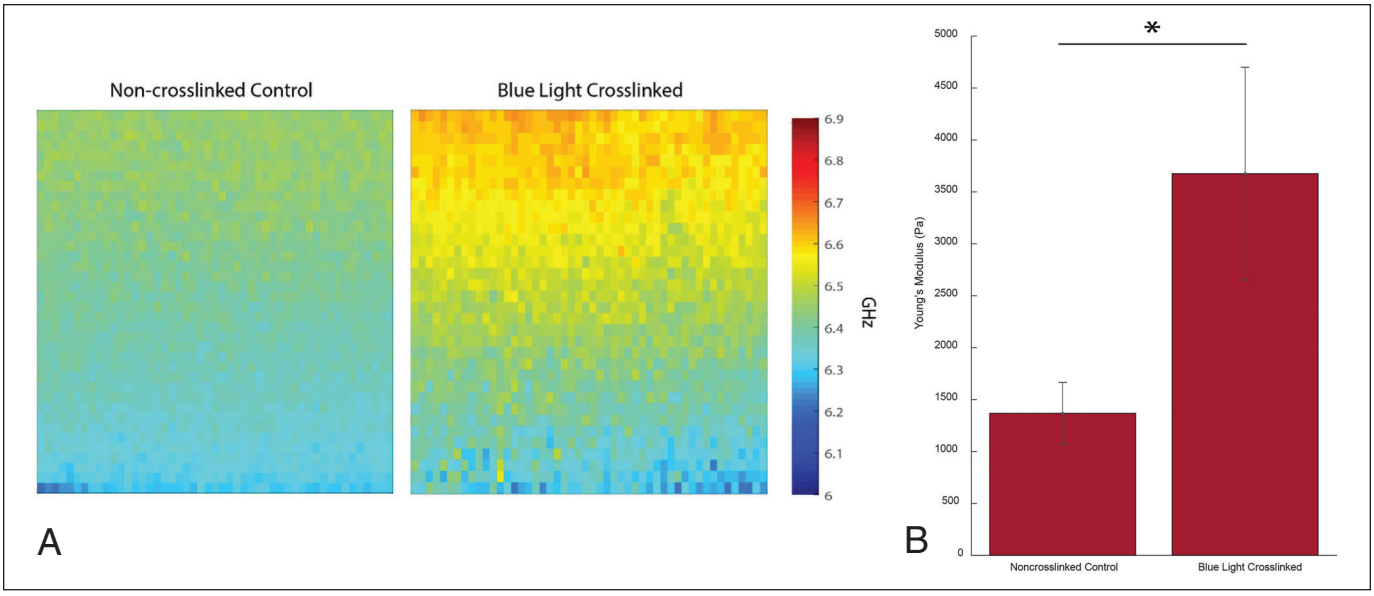

Figure 2. (A) Representative Brillouin maps (4,000 × 700 µm) produced with MATLAB software (Mathworks, Natick, MA) (color map: jet) of both a virgin (control) and a blue light cross-linked porcine cornea positioned anterior up. The cross-linked cornea was exposed to 15 mW/cm^2 blue light for 20 minutes. (B) Bar graph comparing the elasticity, found via Microsquisher (Cellscale, Waterloo, Ontario, Canada) compression, of control corneal punches and cross-linked punches. Error bars represent standard error of the mean for each condition (* = P < .05).

were separated by a remarkably broad transition zone. **Figure 1B**, a transverse profile of the normalized Brillouin modulus, shows an evident transition zone between the cross-linked and non-cross-linked sections.

Figure 2 shows the CXL capabilities of the blue light protocol. Specifically, **Figure 2A** displays representative Brillouin maps of control and blue light cross-linked corneas. To validate the stiffening effects of the blue light protocol, we compared the Microsquisher-derived Young's modulus of control and blue light cross-linked buttons punched from the same respective cornea. As summarized in **Figure 2B**, the blue light cross-linked samples showed a significantly higher Young's modulus ($P \leq .05$) than the untreated controls, yielding a modulus of 3,972.2 ± 1,048 vs 1,419.7 ± 312.8 Pa, respectively (180% the Young's modulus of their respective controls).

Figure 3 quantifies the transition zone induced strictly from the blue light L-CXL optical set-up. The transition zone broadened as the distance between the camera and mask increased from 0 to 500 and 1,000 µm, mimicking the anterior, central, and posterior sections of the porcine cornea, respectively. At its broadest, the transition zone due to illumination was still less than 25 µm.

Figure 4 shows the average normalized transition zone in the blue light cross-linked porcine eyes of 610 µm extending beyond the mask surface.

Figure 5 quantifies the scattering-induced transition zones throughout the cornea during blue light L-CXL. Through just air, therefore without any corneal scattering, a sharp transition zone of 37 ± 8.9 µm was found. This is consistent with **Figure 3** because we had to increase the distance between the mask and camera from 1 to 3 mm, which caused the slight increase in transition zone. In an untreated cornea, the transition zone significantly increased to 102 ± 17.2 µm ($P \leq .01$). The transition zone of the cornea increased even further due to the presence of riboflavin, reaching 159 ± 3.2 µm, a significantly increased transition zone compared to the untreated cornea condition ($P \leq .05$).

A summary of the transition zone findings can be found in the **Table 2**.

DISCUSSION

In this study, we characterized the spatially varying stiffness of the cornea following L-CXL. Biomechanical imaging analysis via Brillouin microscopy demonstrated two distinct regions: a cross-linked area and a non-cross-linked area. The modulus versus depth profile of the cross-linked section mimicked that of a uniformly cross-linked cornea.[28] As expected, the cross-linked section markedly differed from the non-cross-linked section in the anterior region.[9,18,28] The two sections were separated by a broad transition zone. Therefore, the CXL extended farther than the area exposed to light.

To investigate whether the effect was optically induced, we replaced the UV light source with a blue laser to optimize sharpness and set the CXL procedure to replicate the stiffening results of UV CXL. Under the localized protocol, we observed a transition zone of greater than 600 µm even though the blocking mask produced an illumination transition zone through

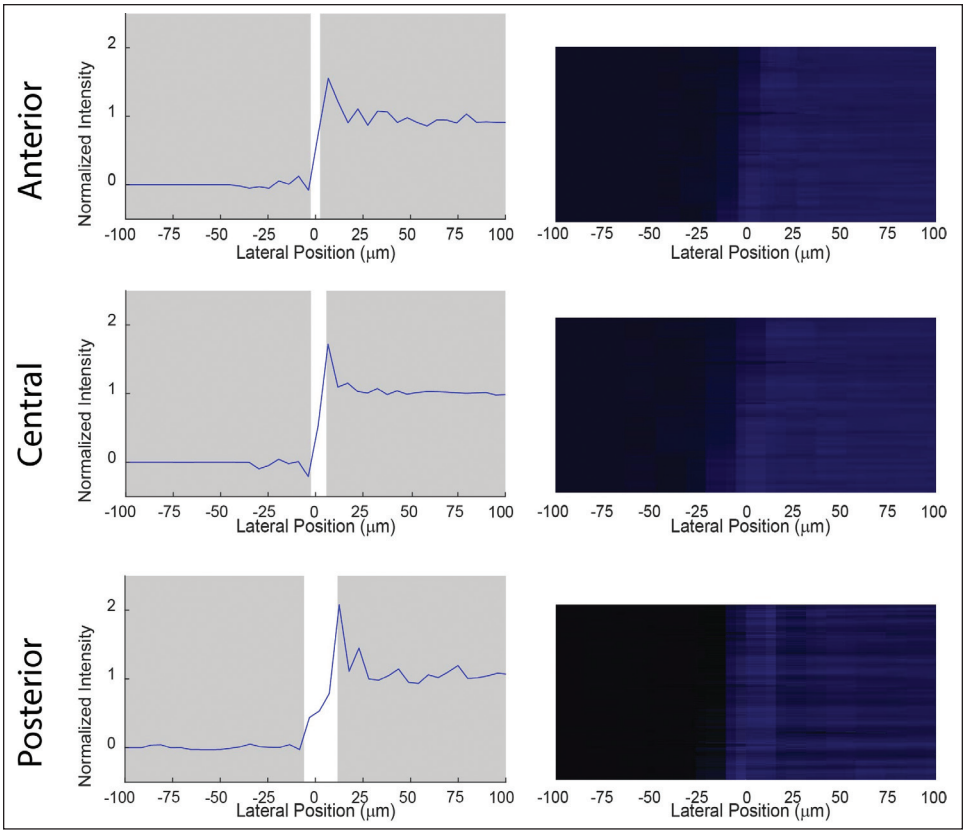

Figure 3. Transition zone and representative light intensity image at anterior (0 μm), central (500 μm), and posterior (1,000 μm) depths from the blocking mask generated from the blue light alone. The normalized light intensity versus lateral position was analyzed using complementary metal–oxide–semiconductor (CMOS) camera (Mightex Systems, Toronto, Ontario, Canada)–captured images at 0, 500, and 1,000 μm between the mask and camera; representing the sharpest possible transition zones through air. Point 0 μm on the horizontal axis was located at 50% normalized intensity. The transition zone at any depth did not exceed 25 μm.

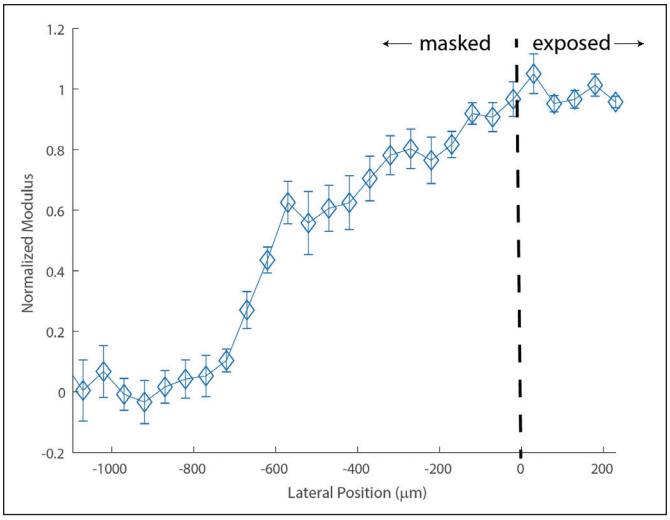

Figure 4. Averaged normalized transition zone of porcine corneas (n = 10) after blue light localized cornal cross-linking. The dotted line illustrates the edge of the ultraviolet blocking mask, differentiating the blocked and exposed sections of the cornea. The average transition zone was calculated between the 10% and 90% of the maximum plateau of normalized modulus. Error bars represent standard error of the mean for each position.

air of less than 25 μm. The broad zone within locally cross-linked corneas must be due to an intrinsic characteristic of the cornea or CXL procedure.

The experiments conducted were on ex vivo porcine corneas. With time, ex vivo corneas become increasingly opaque, therefore becoming more susceptible to light scattering. To validate our findings for future in vivo settings, we measured the scattering effect of the porcine corneas. We found that, at a 3-mm distance from the mask, the corneal transition zone was significantly greater than the illumination transition zone through air. The scattering induced solely by the porcine corneas contributed to roughly 100-μm transition zone and increased further to greater than 150 μm after the corneas were soaked in riboflavin. In vivo corneas have a lower natural scattering property,[29,30] so our results represent the upper boundary of the transition zone one may find in vivo.

Blue light was used in this experimental set-up. At 15 mW/cm^2 for 20 minutes, the blue light stiffened the corneas to 180% of the Young's modulus of their respective controls. This can thus be considered a suitable model to simulate the stiffening of standard CXL protocols performed using UV light.[31] Clinical application calls for columnized UV-A exposure. A clinically used, columnated UV system, creating a well-confined source of light, should produce results similar to those of our set-up. We used a coherent laser for illumination, understanding it to be an ideal optical scenario regarding the transition zone. As expected, the blue coherent light allowed us to obtain sharp confinement of the illumination.

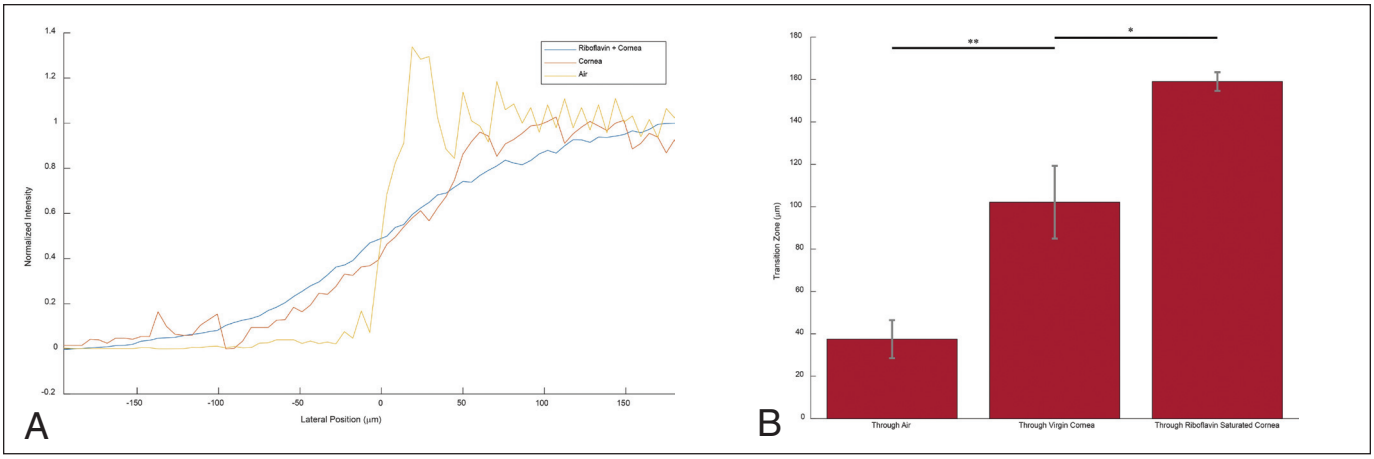

Figure 5. (A) Representative graphs of the normalized light intensity versus lateral position from the 0 point at 50% intensity as the light traveled through air, a virgin cornea, and a riboflavin-soaked cornea to quantify light scattering propagation in each environment. (B) Bar graph representing the average transition zone as light traveled through three distinct environments. Error bars represent standard error of the mean for each condition (* = $P < .05$, ** = $P < .01$).

After considering all of these different factors, we estimated less than 250 μm of the 610-μm transition zone was due to light-related effects. Therefore, as summarized in **Table 2**, a large portion of the transition zone remains unaccounted for by light phenomena. Several factors could be contributing to this effect. The area of CXL depends on the distribution of riboflavin concentration during light exposure, absorbed photons of light, and oxygen exposure to activated riboflavin.[5-8,32] Throughout the 20 minutes of light exposure, there exists a diffusion of oxygen radicals and/or hydrogen peroxide,[33,34] both of which contribute to CXL. Therefore, any diffusion of such reactants could result in the extended CXL area. Furthermore, the cornea becomes increasingly turbid throughout CXL,[35,36] accounting for increased scattering of light as the procedure is performed. Light scattering throughout the process of L-CXL could result in the excitation of riboflavin molecules outside of the irradiated area, subsequently leading to CXL within the transition zone.

L-CXL protocols have garnered added attention recently.[11-13] Seiler et al.[11] employed L-CXL with treatments with customized maximal irradiation ranging from 5.4 up to 10 J/cm^2 centered on the maximum posterior elevation in concentric rings and found improved maximal flattening and corneal regularization at 1 year but unknown long-term stabilization effects. Cassagne et al.[12] performed topography-guided CXL in zonal patterns with total irradiance ranging from 5.4 J/cm^2 in regions surrounding the cone to 15 J/cm^2 on top of the cone using 30 mW/cm^2 pulsed UV-A irradiance and found significant improvements in corrected distance visual acuity, maximum keratometry, mean keratometry in the inferior part of the cornea (I index), and a demarcation line that was more pronounced in maximally treated areas but less pronounced in surrounding regions at 1 year. Nordström et al.[13] used an asymmetrical treatment zone centered on the area of maximum corneal steepness with treatment energies ranging from 7.2 to 15.0 J/cm^2 and found improved visual acuity, spherical refractive error, and maximum keratometry compared to uniformly applied CXL using 5.4 J/cm^2 pulsed fluence.[13]

TABLE 2
Transition Zones Observed From Each Protocol

Protocol	Average Transition Zone (μm)
Blue light L-CXL	610
Light propagation	25
Virgin corneal scattering	102
Riboflavin soaked corneal scattering	159

L-CXL = localized corneal cross-linking

None of these protocols were based on any specific corneal stiffness alteration but rather on the general concept of applying greater irradiation leading to greater stiffness in the maximal cone region and less in surrounding regions. As L-CXL protocols become more sophisticated over time and specific corneal stiffening outcomes are targeted, the biomechanical impact on the transition zone will need to be taken into account during treatment planning.

We found a broad transition zone of approximately 600 μm between the fully cross-linked and non-cross-linked sections of the cornea in L-CXL procedures. Therefore, a stiffening effect exists that extends beyond the irradiated area. We quantified the contribution of light propagation through the cornea, finding it only partially describes the extent of the transition zone. Finally, we validated our transition zones were not due to ex vivo scattering artifacts and therefore are

a result of intrinsic corneal properties. When conducting L-CXL clinically, it will be important to account for increased stiffening outside of the irradiated area.

AUTHOR CONTRIBUTIONS

Study concept and design (JNW, GS); data collection (JNW, EL); analysis and interpretation of data (JNW, FH, JBR, GS); writing the manuscript (JNW, JBR, GS); critical revision of the manuscript (JNW, EL, FH, JBR, GS)

REFERENCES

1. Gain P, Jullienne R, He Z, et al. Global survey of corneal transplantation and eye banking. *JAMA Ophthalmol*. 2016;134:167-173.
2. Scarcelli G, Besner S, Pineda, R, Kalout P, Yun SH. In vivo biomechanical mapping of normal and keratoconus corneas. *JAMA Ophthalmol*. 2015;133:480-482.
3. Ruberti JW, Sinha Roy A, Roberts CJ. Corneal biomechanics and biomaterials. *Annu Rev Biomed Eng*. 2011;13:269-295.
4. Roberts CJ, Dupps WJ Jr. Biomechanics of corneal ectasia and biomechanical treatments. *J Cataract Refract Surg*. 2014;40:991-998.
5. Kymionis GD, Portaliou DM, Diakonis VF, Kounis GA, Panagopoulou SI, Grentzelos MA. Corneal collagen cross-linking with riboflavin and ultraviolet-A irradiation in patients with thin corneas. *Am J Ophthalmol*. 2012;153:24-28.
6. Richoz O, Hammer A, Tabibian D, Gatzioufas Z, Hafezi F. The biomechanical effect of corneal collagen cross-linking (CXL) with riboflavin and UV-A is oxygen dependent. *Trans Vis Sci Technol*. 2013;2:6.
7. Wollensak G, Spoerl E, Seiler T. Riboflavin/ultraviolet-a–induced collagen crosslinking for the treatment of keratoconus. *Am J Ophthalmol*. 2003;135:620-627.
8. Wollensak G, Spoerl E, Seiler T. Stress-strain measurements of human and porcine corneas after riboflavin–ultraviolet-A-induced cross-linking. *J Cataract Refract Surg*. 2003;29:1780-1785.
9. Webb JN, Su JP, Scarcelli G. Mechanical outcome of accelerated corneal crosslinking evaluated by Brillouin microscopy. *J Cataract Refract Surg*. 2017;43:1458-1463.
10. Zhang Y, Conrad AH, Conrad GW. Effects of ultraviolet-A and riboflavin on the interaction of collagen and proteoglycans during corneal cross-linking. *J Biol Chem*. 2011;286:13011-1322.
11. Seiler TG, Fischinger I, Koller T, Zapp D, Frueh BE, Seiler T. Customized corneal cross-linking: one-year results. *Am J Ophthalmol*. 2016;166:14-21.
12. Cassagne M, Pierné K, Galiacy SD, Asfaux-Marfaing MP, Fournié P, Malecaze F. Localized topography-guided corneal collagen cross-linking for keratoconus. *J Refract Surg*. 2017;33:290-297.
13. Nordström M, Schiller M, Fredriksson A, Behndig A. Refractive improvements and safety with topography-guided corneal crosslinking for keratoconus: 1-year results. *Br J Ophthalmol*. 2017;101:920-925.
14. Sachdev GS, Sachdev M. Recent advances in corneal collagen cross-linking. *Indian J Ophthalmol*. 2017;65:787-796.
15. Sinha Roy A, Dupps WJ Jr. Patient-specific computational modeling of keratoconus progression and differential responses to collagen cross-linking. *Invest Ophthalmol Vis Sci*. 2011;52:9174-9187.
16. Wernli J, Schumacher S, Spoerl E, Mrochen M. The efficacy of corneal crosslinking shows a sudden decrease with very high intensity UV light and short treatment time. *Invest Ophthalmol Vis Sci*. 2013;54:1176-1180.
17. Hammer A, Richoz O, Arba Mosquera S, Tabibian D, Hoogewoud F, Hafezi F. Corneal biomechanical properties at different corneal cross-linking (CXL) irradiances. *Invest Ophthalmol Vis Sci*. 2014;55:2881-2884.
18. Scarcelli G, Pineda R, Yun SH. Brillouin optical microscopy for corneal biomechanics. *Invest Ophthalmol Vis Sci*. 2012;53:185-190.
19. Kashiwabuchi RT, Quinto GG, Castro-Combs J, Behrens A. Corneal collagen cross-linking with riboflavin/lumiflavin and blue light (5450nm) to reduce posterior lamellar dislocation in endothelium keratoplasty. *Invest Ophthalmol Vis Sci*. 2009;50:5495.
20. Scarcelli G, Polacheck WJ, Nia HT, et al. Noncontact three-dimensional mapping of intracellular hydromechanical properties by Brillouin microscopy. *Nat Methods*. 2015;12:1132-1134.
21. Scarcelli G, Yun SH. Confocal Brillouin microscopy for three dimensional mechanical imaging. *Nature Photonics*. 2007;9:39-43.
22. Scarcelli G, Yun SH. Multistage VIPA etalons for high-extinction parallel Brillouin spectroscopy. *Opt Exp*. 2011;19:10913-10922.
23. Berghaus KV, Yun SH, Scarcelli G. High speed sub-GHz spectrometer for Brillouin scattering analysis. *J Vis Exp*. 2015;(106):e53468.
24. Kikkawa Y, Hirayama K. Uneven swelling of the corneal stroma. *Invest Ophthalmol*. 1970;9:735-741.
25. Aldahlawi NH, Hayes S, O'Brart DPS, Meek KM. Standard versus accelerated riboflavin–ultraviolet corneal collagen crosslinking: resistance against enzymatic digestion. *J Cataract Refract Surg*. 2015;41:1989-1996.
26. McCall AS, Kraft S, Edelhauser HF, et al. Mechanisms of corneal tissue cross-linking in response to treatment with topical riboflavin and long-wavelength ultraviolet radiation (UVA). *Invest Ophthalmol Vis Sci*. 2010;51:129-138.
27. Wollensak G, Spoerl E, Wilsch M, Seiler T. Keratocyte apoptosis after corneal collagen cross-linking using riboflavin/UVA treatment. *Cornea*. 2004;23:43-49.
28. Scarcelli G, Kling S, Quijano E, Pineda R, Marcos S, Yun SH. Brillouin microscopy of collagen crosslinking: noncontact depth-dependent analysis of corneal elastic modulus. *Invest Ophthalmol Vis Sci*. 2013;54:1418-1425.
29. Olsen T. Light scattering from the human cornea. *Invest Ophthalmol Vis Sci*. 1982;23:81-86.
30. Spadea L, Maraone G, Verboschi F, Vingolo EM, Tognetto D. Effect of corneal light scatter on vision: a review of the literature. *Int J Ophthalmol*. 2016;9:459-464.
31. Seifert J, Hammer CM, Rheinlaender J, et al. Distribution of Young's modulus in porcine corneas after riboflavin/UVA-induced collagen cross-linking as measured by atomic force microscopy. *PloS One*. 2014;9:e88186.
32. Roberts CJ, Dupps WJ Jr, Downs JC. *Biomechanics of the Eye*. Wayne, PA: Kugler Publications; 2018.
33. Wilson G, Riley MV. Does topical hydrogen peroxide penetrate the cornea. *Invest Ophthalmol Vis Sci*. 1993;34:2752-2760.
34. Chalmers RL. A review of the metabolism of hydrogen peroxide by external ocular structures. *Int Contact Lens Clin*. 1995;22:143-147.
35. Beckman Rehnman J, Janbaz CC, Behndig A, Lindén C. Spatial distribution of corneal light scattering after corneal collagen crosslinking. *J Cataract Refract Surg*. 2011;37:1939-1944.
36. Wollensak G, Wilsch M, Spoerl E, Seiler T. Collagen fiber diameter in the rabbit cornea after collagen crosslinking by riboflavin/UVA. *Cornea*. 2004;23:503-507.